

STUDIES OF MULTISTEM DRIFT TUBE ACCELERATOR STRUCTURES\*

S. Giordano and J.P. Hannwacker  
Brookhaven National Laboratory  
Upton, New York

Introduction

The Alvarez-type drift tube structure, operating in the  $TM_{010}$  mode, has been used for accelerating protons below energies of 60 MeV. It has been shown by many investigators that the high shunt impedance of the Alvarez-type structure merits the use of such a structure for energies up to 150 or 200 MeV. The disadvantage of an Alvarez structure is the fact that the  $TM_{010}$  is a zero order mode which is located at the end of a passband, where the group velocity ( $v_g = |dw/d\beta| = 0$ ) is zero, resulting in a structure that is sensitive to amplitude and phase distortion as a function of beam loading, RF power excitation,<sup>1</sup> and detuning effects.

Theory

Let us first consider three possible structures that are used for accelerating protons, the "0", " $\pi/2$ " and " $\pi$ " mode configurations. Various investigators have discussed the relative merits of the above-mentioned structures. To reduce beam loading and tank detuning effects it is desirable to do either of the following:

1) For the 0 or  $\pi$  mode structure to make the quantity  $|d^2\omega/d\beta^2|$  as large as possible (noting that for the 0 or  $\pi$  mode  $|dw/d\beta| = 0$ ).

2) For the  $\pi/2$  mode structure (which is normally located at the center of a passband) to make the quantity  $|dw/d\beta|$  as large as possible.

It has been shown<sup>2-5</sup> that the use of one or more stems to support a drift tube plays a significant role in shaping the dispersion curve about the operating  $TM_{010}$  mode, due to the existence of a transverse stem resonance. These transverse stem resonances result in a set of  $TS(N)_{nm\ell}$  modes, and it is these modes that are responsible for changing the dispersion curve about the operating  $TM_{010}$  accelerating mode. It is possible to not only increase  $|d^2\omega/d\beta^2|$  about the operating mode, but to actually make  $|dw/d\beta|$  finite, which is equivalent to the operating characteristics of a  $\pi/2$  mode structure.

Experimental Results

Measurements were carried out on a cylindrical cavity having a length of 36 in. and a diameter of 10.8 in. Of particular interest for the present discussion are the  $TM_{01\ell}$  and  $TE_{11\ell}$  modes. Figure 1

is a plot of these modes for the hollow unloaded cavity. It should be noted that there are no modes below 650 Mc/s (650 Mc/s is the lowest frequency that energy can propagate down this structure for the above-mentioned modes).

Figure 2 shows a drift tube structure having a single stem support for each drift tube. This structure is scaled down from 200 Mc/s for operation at a  $\beta \approx 0.43$ . The modes of this cavity were measured and are shown in Fig. 3. A comparison between Figs. 1 and 3 reveals a number of interesting differences. The addition of a single stem and drift tube decreases the frequency spacing between the  $TE_{11\ell}$  and  $TM_{01\ell}$  modes, and in addition introduces a new set of modes which we shall call the  $TS(1)_{10\ell}$  modes. For modes designated  $TS(N)$ ,  $N$  indicates the number of stems, and the subscripts are the usual  $\phi$ ,  $r$ , and  $z$  cylindrical coordinates. It should be pointed out that the  $TS$  modes are similar to those mentioned in the literature for the crossbar<sup>6,7</sup> and for the H-type<sup>8</sup> wave structure.

Now consider the structure shown in Fig. 4, which is the same as that shown in Fig. 2, with the exception that there are two stems  $180^\circ$  apart. Figure 5 is a plot of the  $TM_{01\ell}$ ,  $TE_{11\ell}$  and  $TS(2)_{10\ell}$  modes for the two stem case. It is interesting to note that there is very little change in either the  $TM_{01\ell}$  or the  $TE_{11\ell}$  modes, as compared to the single stem case, but the  $TS(2)_{10\ell}$  modes are higher in frequency than the  $TS(1)_{10\ell}$  modes.

Similar measurements were made on 3, 4 and 6 stem structures with configurations shown in Fig. 6. For the 3, 4 and 6 stem cases it was found that all the  $TE_{11\ell}$  modes were above 1200 Mc. The results for the  $TM_{01\ell}$  and  $TS(N)_{10\ell}$  modes for the 1, 2, 3, 4 and 6 stem cases are compiled in Fig. 7.

In Fig. 7 it is seen that for the one and two stem case the  $TM_{01\ell}$  bandpass remains relatively unaffected by the  $TS(N)_{10\ell}$  bandpass. In going to 3, 4 or 6 stems the  $TM_{01\ell}$  bandpass is influenced by the  $TS(N)_{10\ell}$  bandpass. At some region between 4 and 6 stems it may be possible to have the  $TS(N)_{10\ell}$  and  $TM_{01\ell}$  bandpasses join together and form a continuous dispersion curve, in which case the behavior of the  $TM_{010}$  mode would be more like that of a  $\pi/2$  mode.

The six stem case, as shown in Fig. 7, is obviously an overcompensated case and will not be discussed in this paper. The four stem case is obviously undercompensated. It has been shown,<sup>2,3,5</sup> that the frequency of the  $TS(N)$  modes can be changed by changing the stem diameters. Figure 8 shows the resulting dispersion curves for the four stem configuration, having various stem diameters. From Fig. 8 we see that for the four stem case having a diameter of  $3/4$  in, we get the two dispersion curves

\*Work performed under the auspices of the U.S. Atomic Energy Commission.

(TM and TS) to form what appears to be a continuous dispersion curve.

A second set of measurements were made on a scaled-down cavity, having 6 drift tubes, at a  $\beta = 0.4$  (84 MeV). The results of these measurements are shown in Fig. 9. For the single stem case two sets of measurements were made, one where all the stems were in line, and the second where alternate pairs of stems were rotated  $90^\circ$  from each other. We see essentially no change in the dispersion curves for the above two cases. For the two stem case, each drift tube has two stems  $180^\circ$  apart. Shown in Fig. 9 for the two stem case we have two sets of measurements, one where all the stems were in a common plane, and the second where alternate pairs of stems were rotated  $90^\circ$  from each other. Here again we see that there is essentially no change in the dispersion curves. It should be pointed out that the above measurements were made at 84 MeV, but at lower energies rotating adjacent drift tube stems should increase the bandwidth of the TS(N) passband.

Figure 9 also shows the dispersion curves of the 3 and 4 stem configurations. For the four stem case we see that the two dispersion curves [the TM and TS(N)] appear to form one continuous dispersion curve. We now want to determine how close these two dispersions match up, by comparing the resonant frequency of the  $TM_{010}$  and  $TS(N)_{100}$  modes.

#### Determining the $TS(N)_{100}$ Resonance

Let us first consider the usual types of TM and TS(N) dispersion curves as shown in Fig. 10. Because of the end walls on a cavity the  $TS(N)_{100}$  mode cannot be excited. We would like to be able to measure the  $TS(N)_{100}$  resonant frequency to determine how closely we have matched the two dispersion curves. Let us first consider a single drift tube, supported by any stem configuration, in the center of a long hollow open-ended cylindrical cavity. The drift tube and stem(s) will have a transverse TS(N) resonant frequency. The frequency of the TS(N) resonance is below the cut-off frequency of the cylinder and, as such, the fields will decay rapidly. We note that the above resonance represents a perturbed  $TS(N)_{100}$  mode, the reason being that the cut-off waveguide section only approximates the field at the end plate boundaries that we are replacing with the cut-off waveguide section. If we say that the actual  $TS(N)_{100}$  resonant frequency is  $f_0$  and  $U_0$  the stored energy, and since the cut-off waveguide perturbs the stored energy of the boundary fields by an amount  $\Delta U$ , we may write the simple frequency perturbation relationship

$$\frac{\Delta f_1}{f_0} = \frac{\Delta U}{2U_0},$$

where  $\Delta f_1$  is the change in the resonant frequency. If we now put two drift tubes into the open-ended cavity, we get

$$\frac{\Delta f_2}{f_0} = \frac{\Delta U}{2 \times U_0} = \frac{\Delta U}{4U_0},$$

where we have assumed that the stored energy doubles (since there are two drift tubes), but the perturbation caused at the boundary by the cut-off waveguide section remains unchanged. We may now write the following expression for  $n$  drift tubes

$$\frac{\Delta f_n}{f_0} = \frac{\Delta U}{2nU_0}. \quad (1)$$

If  $f'_n$  is the measured frequency for  $n$  drift tubes, we now write

$$f'_n = f_0 + \Delta f_n. \quad (2)$$

From (1) and (2) we get

$$f'_n = f_0 - \frac{f_0 \Delta U}{2nU_0}. \quad (3)$$

In Eq. (3)  $f_0$ ,  $\Delta U$  and  $U_0$  are all constants, therefore if we plot the measured frequency  $f'_n$  vs.  $1/n$  we should get a straight line, as shown in Fig. 11 and the intercept with the abscissa should be the value of  $f_0$ , which is the unperturbed  $TS(N)_{100}$  mode. (It should be noted, in Fig. 11, that the points corresponding to  $n = 2, 3, 4, 5$ , and  $6$  are indeed on a straight line. The point  $n = 1$  is off due to the fact that the end perturbation represents a large effect on the stored energy of a single drift tube, as compared to the stored energy of more than one drift tube. It should be pointed out that if similar measurements are made on a structure having lower  $\beta$ 's than the above structure, it may be necessary to measure a greater number of drift tubes in order to arrive at the straight line portion of the curve as shown in Fig. 11.)

#### Conclusions

From Fig. 11, we see that for the four stem case we get a  $TS(N)_{100}$  mode frequency of 795 Mc. For the same case, as shown in Fig. 9, the  $TM_{010}$  mode frequency is 830 Mc. We see that there is an actual gap between the TM and TS(N) dispersion curves of 35 Mc. Even with this gap, the TM dispersion curve, about the  $TM_{010}$  mode, shows a considerable improvement in that the spacing between the  $TM_{010}$  and  $TM_{011}$  modes for the one stem case is only 14 Mc, while for the four stem case the spacing between these two modes is 60 Mc. As was shown<sup>3</sup> even with the above gap between the two dispersion curves, there was as much as a factor of 10 improvement in the reduction of tank detuning effects. We may improve the structure even further by closing the gap between the two dispersion curves, by simply increasing the diameter of the stems.

#### References

1. S. Giordano, J.P. Hannwacker, and J.T. Keane, "Studies of Multi-Drive Excitation for Alvarez Structures," to be published in the Proceedings of this Conference.

2. S. Giordano, "Measurements on the Multi-Stem Drift-Tube Structure for Proton Accelerators," BNL Accelerator Dept. Internal Report AGSCD-11, June 22, 1966.
3. S. Giordano and J.P. Hannwacker, "Measurement on a Multistem Drift Tube Structure," Proc. 1966 Linear Accelerator Conference, Los Alamos, p. 88 (CFSTI, Springfield, Virginia, 1966).
4. T. Nishikawa, "Equivalent Circuit and Dispersion Relation for the Multistem Drift Tube Structure," BNL Accelerator Dept. Internal Report AADD-125, November 18, 1966.
5. S. Giordano, "A New Multi-Stem, Drift-Tube, Standing-Wave, Zero-Mode Proton Accelerating Structure," BNL Accelerator Dept. Internal Report AGSCD-7, February 25, 1966.
6. A. Carne and N. Fewell, "P.L.A. Report 1962," NIRL/R/24, Rutherford High Energy Laboratory.
7. A. Carne and N. Fewell, "P.L.A. Progress Report 1963," NIRL/R/60, Rutherford High Energy Laboratory.
8. P.M. Zeidlits and V.A. Yamnitskii, "Accelerating Systems Employing H-Type Waves," Plasma Physics 4, 121 (1962).

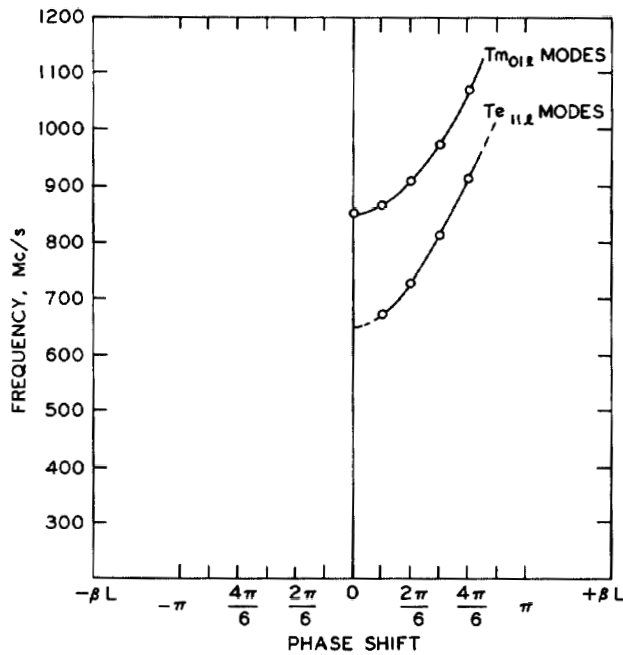


Fig. 1. Hollow cylindrical cavity.

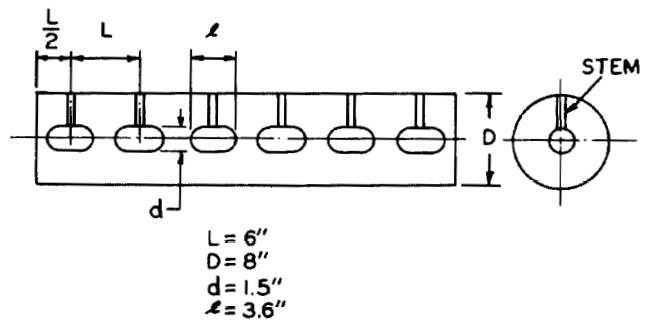


Fig. 2. Single stem drift tube cavity.

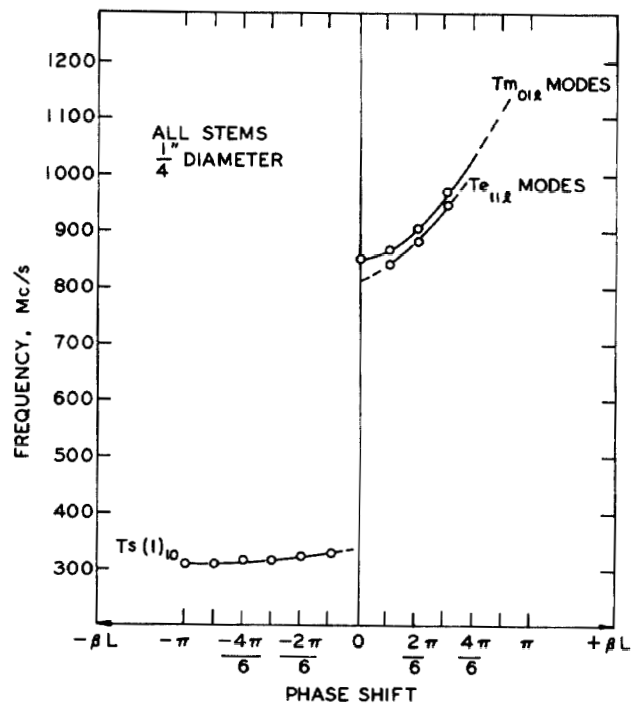


Fig. 3. Modes of the single stem drift tube cavity.

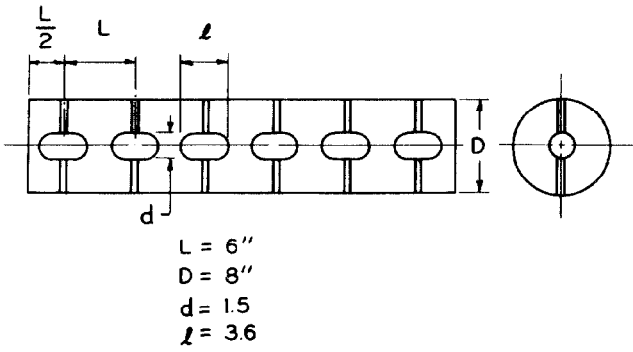


Fig. 4. Two stem ( $180^\circ$ ) drift tube cavity.

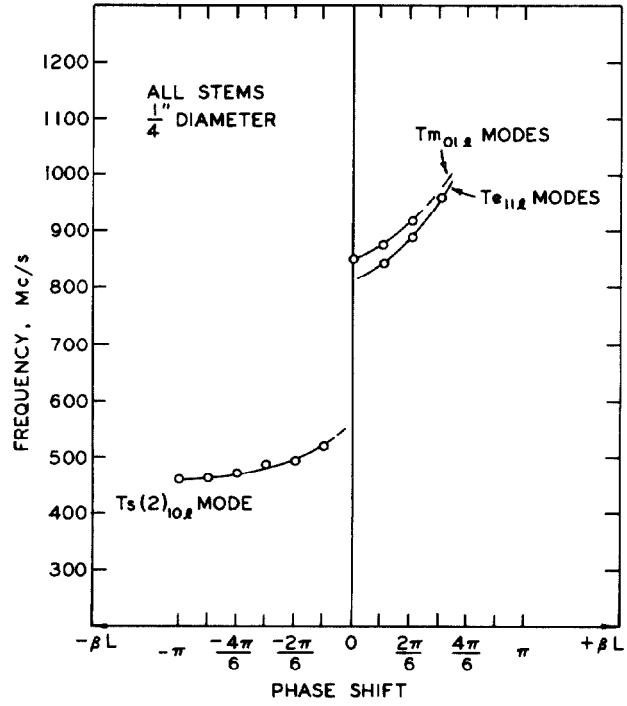


Fig. 5. Modes of the two stem ( $180^\circ$ ) drift tube cavity.

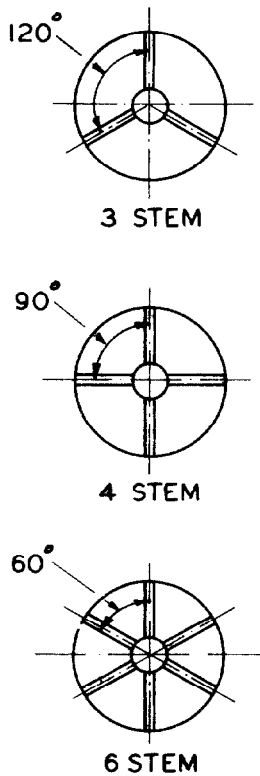


Fig. 6. Multistem configurations.

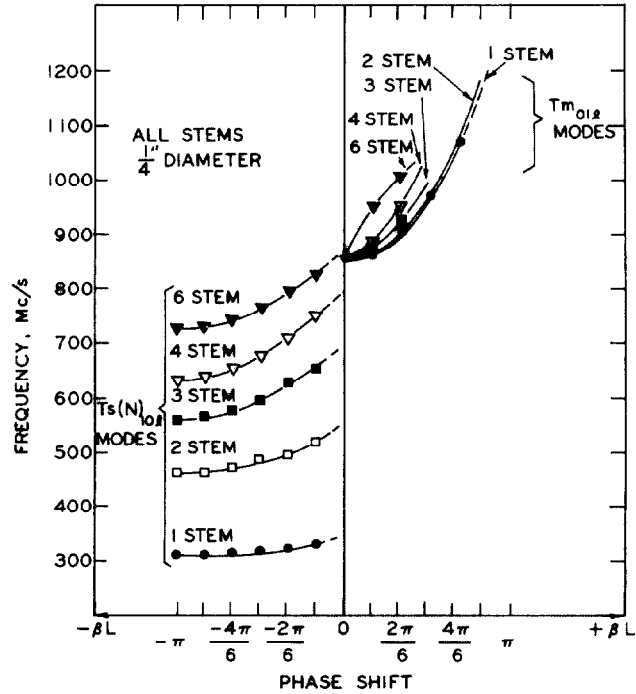


Fig. 7. Modes of multistem drift tube cavities.

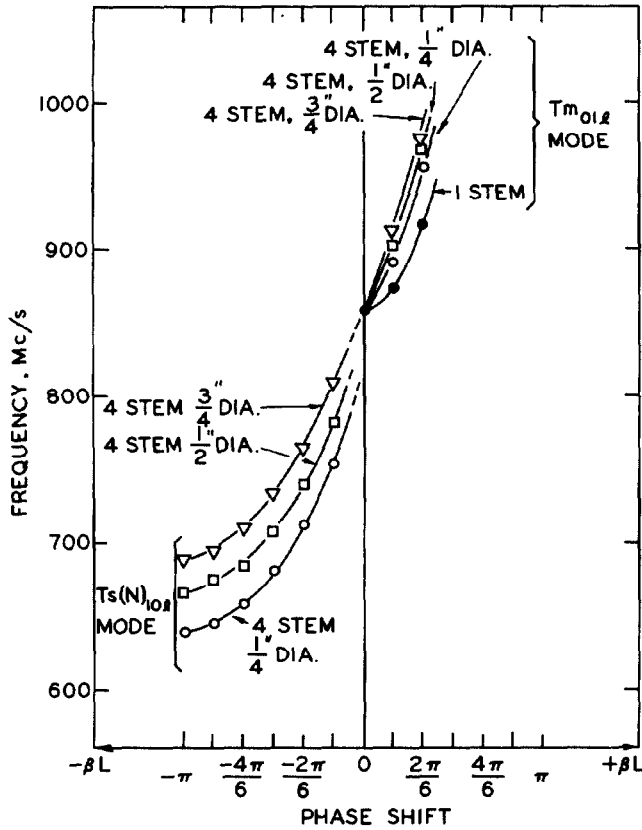


Fig. 8. Four stems with various diameters.

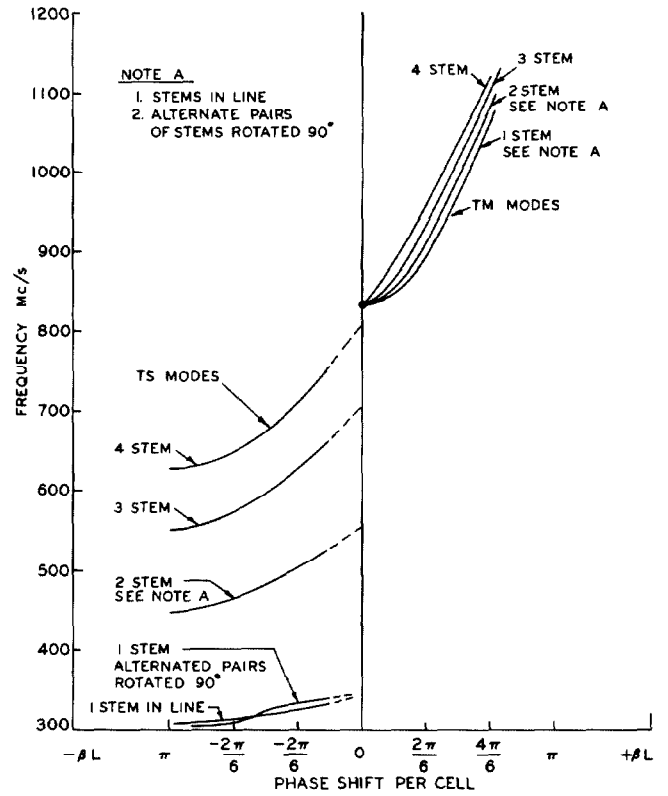


Fig. 9. Dispersion curve for a multistem drift tube 84 MeV Alvarez structure (6 drift tube assembly).

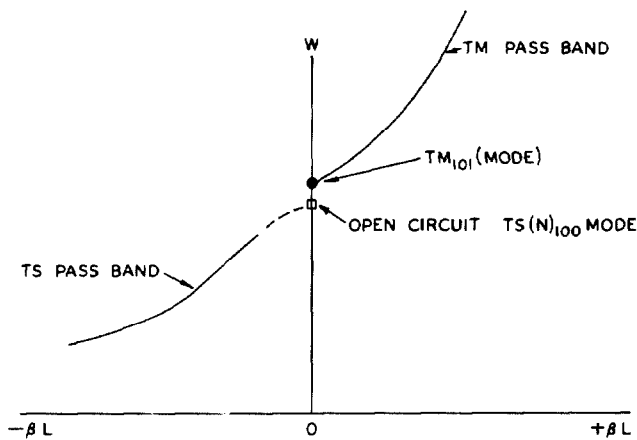


Fig. 10. A typical dispersion characteristic for stem supported drift tubes.

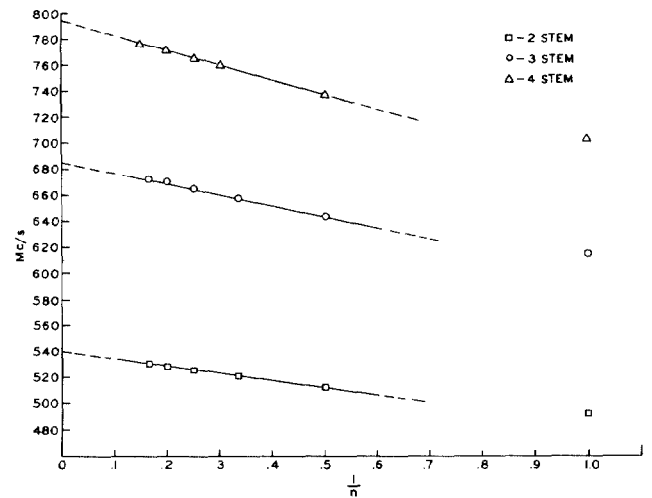


Fig. 11. Frequency of  $Ts(N)_{100}$  mode vs.  $1/n$  (where  $n$  = number of drift tubes).